HHS Public Access

Author manuscript

Immunity. Author manuscript; available in PMC 2018 April 18.

Published in final edited form as:

Immunity. 2017 April 18; 46(4): 635–648. doi:10.1016/j.immuni.2017.03.014.

SYK licenses MyD88 to instigate IL-1α-mediated inflammatory disease

Prajwal Gurung[1,5], **Gaofeng Fan**[2,5], **John R. Lukens**[3], **Peter Vogel**[4], **Nicholas K Tonks**[2], and **Thirumala-Devi Kanneganti**[1,6,*]

[1]Department of Immunology, St. Jude Children's Research Hospital, Memphis, TN, 38105, USA

[2]Cold Spring Harbor Laboratory, Cold Spring Harbor, NY, 11724, USA

[3]Center for Brain Immunology and Glia (BIG), Department of Neuroscience, University of Virginia, Charlottesville, VA, 22908, USA

[4]Animal Resources Center and the Veterinary Pathology Core, St. Jude Children's Research Hospital, Memphis, TN, 38105, USA

SUMMARY

Mice carrying a hypomorphic point mutation in the *Ptpn6* gene (*Ptpn6*^{spin} mice) develop an inflammatory skin disease that resembles neutrophilic dermatosis in humans. Here, we demonstrated that interleukin (IL)-1α signaling through IL-1R and MyD88 in both stromal and immune cells drive inflammation in *Ptpn6*^{spin} mice. We further identified SYK as a critical kinase that phosphorylates MyD88, promoted MyD88-dependent signaling and mediates dermatosis in *Ptpn6*^{spin} mice. Our studies further demonstrated that SHP1 encoded by *Ptpn6* binds and suppresses SYK activation to inhibit MyD88 phosphorylation. Downstream of SHP1 and SYK-dependent counterregulation of MyD88 tyrosine phosphorylation, we have demonstrated that the scaffolding function of receptor interacting protein kinase 1 (RIPK1) and tumor growth factor-β activated kinase 1 (TAK1)-mediating signaling were required to spur inflammatory disease. Overall, these studies identify SHP1 and SYK crosstalk as a critical regulator of MyD88 post-translational modifications and IL-1-driven inflammation.

Graphical abstract

*Correspondence should be addressed to: Thirumala-Devi Kanneganti, Department of Immunology, St. Jude Children's Research Hospital, MS #351, 570, St. Jude Place, Suite E7004, Memphis TN 38105-2794, Tel: (901) 595-3634; Fax. (901) 595-5766. Thirumala-Devi.Kanneganti@StJude.org.

[5]Contributed equally;

[6]Lead contact;

AUTHOR CONTRIBUTIONS

P.G., G.F., N.K.T., and T.-D.K. designed the study; P.G., G.F. and J.R.L. performed experiments. P.V. assisted with histology. P.G., G.F., N.K.T., and T.-D.K. analyzed data. P.G. and T.-D.K. wrote the manuscript with input from the other authors. T.-D.K. oversaw the project.

CONFLICT OF INTEREST

The authors declare no competing financial interests.

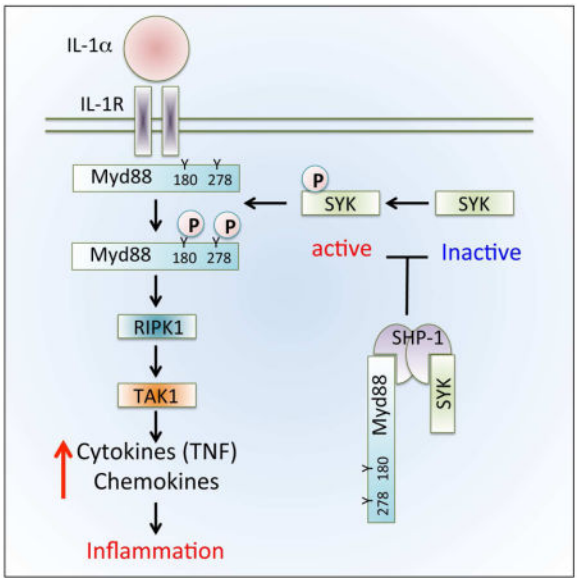

Keywords

SHP1; *Ptpn6*; SYK; IL-1α; IL-1β; MyD88; RIPK1; RIPK3; necrosis; autoinflammation; TAK1; myeloid cells; MLKL

INTRODUCTION

Mutations in the *PTPN6* gene that encodes for the protein tyrosine phosphatase Src homology region 2 domain-containing phosphatase-1 (SHP-1) have been linked with autoinflammatory and autoimmune diseases in humans (Cao and Hegele, 2002; Christophi et al., 2008). Several mouse models with mutations in the *Ptpn6* gene have been described and present with very severe autoinflammatory syndromes as described in the humans (Croker et al., 2008; Green and Shultz, 1975; Shultz et al., 1984; Shultz et al., 1993; Tsui et al., 1993). Motheaten mice (a recessive mutation of *Ptpn6* gene resulting in motheaten phenotype, $Ptpn6^{me/me}$), first described in 1975, have deletion of a cytosine (C) nucleotide in position 228 of the *Ptpn6* gene resulting in complete deletion of full normal SHP-1 (Green and Shultz, 1975; Wishcamper et al., 2001), although other splice variants of SHP-1 have been reported to be functional in these mice (Martin et al., 1999). $Ptpn6^{me/me}$ mice exhibit severe dysfunction of the immune system, develop inflammatory lesions with neutrophil infiltration and die around 3–4 weeks of age (Green and Shultz, 1975; Wishcamper et al., 2001). Motheaten-viable mice (a hypomorphic allele due to a T-to-A transversion at a splice consensus site, $Ptpn6^{me\text{-}v/me\text{-}v}$ mice) also develop myeloproliferative disease and die around 9-10 weeks of age (Shultz et al., 1984; Tsui et al., 1993). While these mouse models have demonstrated critical roles for SHP1 in various immune cells, the premature death of these mice has hindered complete characterization of SHP-1 in the context of inflammatory diseases.

Recent characterization of a hypomorphic *Ptpn6*-mutant mouse with homozygous Tyr208Asn amino acid mutation (exhibits spontaneous inflammation (spin) and referred to

as *Ptpn6*^{spin} mice here) has uncovered a critical role of SHP-1 in regulating inflammatory disorders. *Ptpn6*^{spin} mice display a similar myeloproliferative disorder and footpad inflammation as the motheaten mice; however, unlike the motheaten mice, *Ptpn6*^{spin} mice survive into adulthood (Croker et al., 2008). Moreover *Ptpn6*^{spin} mice develop persistent footpad swelling and suppurative inflammation that is very similar to neutrophilic dermatosis in humans (Croker et al., 2008; Nesterovitch et al., 2011). While the essential roles of interleukin (IL)-1 in promoting these autoinflammatory diseases are well established, it is only recently that the specific roles for IL-1α and IL-1β have been recognized (Lukens et al., 2014; Lukens et al., 2013). Using *Ptpn6*^{spin} mice as a model of inflammatory disease, we previously showed that IL-1α, but not IL-1β or the caspase-1-associated inflammasome is a central cytokine that promotes neutrophilic footpad inflammation (Lukens et al., 2013). Mechanistically, RIPK1 has been shown to regulate IL-1α expression independently of RIPK3, suggesting a role for RIPK1 and IL-1α signaling axis in driving footpad inflammation (Lukens et al., 2013). Several studies including ours have demonstrated that hematopoietic or neutrophil specific deletion of *Ptpn6* is sufficient to promote neutrophilic footpad inflammation (Abram et al., 2013; Lukens et al., 2013). However, the precise molecular events downstream of IL-1α as well as how RIPK1 instigates footpad inflammation provoked by the *Ptpn6*^{spin} *(or* SHP1-deficient) myeloid cells are unknown. More importantly, the regulatory functions of SHP1 remain completely uncharacterized. Thus, understanding the molecular mechanisms of RIPK1 and IL-1α signaling axis, and SHP1 functions that regulates inflammation is required.

Here, we have characterized the molecular underpinnings of RIPK1-dependent control of autoinflammatory disease and established the role for tumor necrosis factor (TNF) downstream of IL-1α that drive inflammatory disease. We have shown that the RIPK1 scaffolding function, but not it's kinase activity or necroptosis promoted disease in *Ptpn6*^{spin} mice. Mechanistically, we established that TAK1 in myeloid cells were critical to provoke this neutrophilic disorder suggesting a role for RIPK1 and TAK1 signaling axis. We further report that spleen tyrosine kinase (SYK) is a critical kinase that is centrally required for the instigation of inflammatory disease in *Ptpn6*^{spin} mice. We also characterized and elucidated SHP1-mediated regulation of SYK activation in controlling MyD88 phosphorylation as a prominent mechanism that controls autoinflammation and skin disease in *Ptpn6*^{spin} mice.

RESULTS

Ptpn6^{spin} mutation in the non-hematopoietic compartment is dispensable for inflammatory disease

IL-1 receptor signaling and MyD88 are centrally required for provoking inflammation and inflammatory skin disease in *Ptpn6*^{spin} mice (Croker et al., 2008; Lukens et al., 2013). To validate this causal mechanism in another *Ptpn6*-driven disease model, we generated mice with a myeloid-specific deletion of *Ptpn6* by breeding *Ptpn6*$^{fl/fl}$ mice with *Lyz2*$^{cre+}$ mice. *Ptpn6*$^{fl/fl}$× *Lyz2*$^{cre+}$ mice with a myeloid-specific deletion of SHP1 developed skin disease with same kinetics as that of *Ptpn6*^{spin} mice and presented with similar extent of inflammation and histologic lesions (Figure 1A–B and Table S1). In addition, the monocyte and neutrophil populations noted in *Ptpn6*^{spin} mice (Lukens et al., 2013) were also elevated

in *Ptpn6*$^{fl/fl}$ × *Lyz2*$^{cre+}$ mice relative to those of their littermate controls (Figure 1C). These studies confirm that SHP1 deficiency in myeloid cells is sufficient to drive this autoinflammatory disease, which is in line with previously published results (Abram et al., 2013; Lukens et al., 2013).

To further delineate how SHP1 deficiency in myeloid cells drives progression of disease, bone marrow chimeras of *Ptpn6*^{spin} and WT mice were generated and examined (Figure 1D–E). Following chimerism, as expected, WT ≫ WT did not develop disease, whereas *Ptpn6*^{spin} ≫ *Ptpn6*^{spin} chimeras developed severe footpad inflammation. All *Ptpn6*^{spin} ≫ WT chimeras developed footpad inflammation as expected, whereas pre-diseased *Ptpn6*^{spin} mice that received WT bone marrow cells (WT ≫ *Ptpn6*^{spin} chimeras) were completely protected. These studies further support the hypothesis that SHP1 deficiency in the hematopoietic compartment (i.e. myeloid cells) is necessary and sufficient for the development of autoinflammatory skin disease, whereas SHP1 disruption in the radioresistant compartment is dispensable.

Radioresistant IL-1α signal via IL-1R in both compartments to drive the inflammatory disease

With the insight that SHP-1-deficiency in disease progression could be compartmentalized to hematopoietic cells, we examined whether IL-1α could also be compartmentalized to either the hematopoietic or radioresistant compartment. IL-1α is an alarmin that stimulates wound-healing responses (Chen et al., 2007; Cohen et al., 2010; Rider et al., 2011), and since inflammation in *Ptpn6*^{spin} mice is mainly confined to the hind footpads, we proposed that IL-1α is released by footpad radioresistant cells during normal wound healing responses. Indeed, wound-healing experiments have shown that IL-1α amounts are highly elevated following microabrasion injury (Lukens et al., 2013). To this end, we generated specific *Ptpn6*^{spin} chimeras to examine the role of stromal IL-1α in the progression of footpad inflammation (Figure 2A). *Ptpn6*^{spin} ≫ *Il1a*$^{-/-}$ chimera mice were completely protected from disease progression (Figure 2A). In contrast, bone marrow cells from protected *Ptpn6*^{spin} ≫ *Il1a*$^{-/-}$ mice, when transferred to WT recipients promoted disease, which further underscores the requirement of IL-1α in the radioresistant but not the hematopoietic compartment (Figure 2B). These findings reveal crosstalk between radioresistant and hematopoietic compartments whereby SHP1-deficient myeloid cells overreact to the release of IL-1α by radioresistant cells during injury, which ultimately results in a self-perpetuating inflammatory skin disease.

IL-1R-mediated signaling was required for disease development (Figure S1A). To examine how IL-1α is perceived by the immune system to promote disease in *Ptpn6*^{spin} mice, we generated chimeras with *Ptpn6*^{spin} and *Il1r1*$^{-/-}$ mice. Our results demonstrated that IL-1R was important in both the radioresistant and hematopoietic compartment for induction of disease in *Ptpn6*^{spin} mice (Figure 2C and D). Altogether, these results suggest that IL-1α produced by radioresistant cells need to signal in both radioresistant cells, as well as immune cells, to promote disease.

Microbiota promotes footpad inflammation in *Ptpn6*^{spin} mice

In addition to the normal damage and repair process (that is potentially driven by IL-1α (Chen et al., 2007; Cohen et al., 2010; Rider et al., 2011)), the footpads are also in constant contact with commensal microorganisms, which may contribute to the modulation of IL-1α expression in stromal cells. Furthermore, several studies have shown that skin-specific commensal microbiota are involved in immunity (Naik et al., 2015; Naik et al., 2012). Thus, we speculated that microbiota could influence disease progression in *Ptpn6*^{spin} mice. Indeed, our studies analyzing 16S ribosomal RNA (rRNA) metagenomic sequencing of intestinal microbiome showed that the microbial landscape was altered in *Ptpn6*^{spin} mice (Figure S2A and B). To investigate the potential role of microbiota in promoting *Ptpn6*^{spin}-mediated inflammatory disease, pre-diseased *Ptpn6*^{spin} mice were administered full spectrum antibiotics (ABX). Whereas all *Ptpn6*^{spin} mice on untreated water developed footpad inflammation before day 100, *Ptpn6*^{spin} mice on ABX water were protected and showed no disease (Figure S2C). Taken together, it could be postulated that microbiota primes IL-1α expression in radioresistant compartment, which when released can promote inflammatory disease in *Ptpn6*^{spin} mice.

IL-1α-induced TNF contributes to inflammatory disease in *Ptpn6*^{spin} mice

Myeloid cells, specifically neutrophils are hyperactivated in *Ptpn6*^{spin} mice and produce exacerbated amounts of pro-inflammatory cytokines such as G-CSF, KC and IL-6 (Lukens et al., 2013). Furthermore, we previously showed that microabrasion injury promotes IL-1α secretion and disease induction in *Ptpn6*^{spin} mice (Lukens et al., 2013). We used this experimental setup to determine the apical cytokines instigating the inflammatory cascade. WT footpads that were microabrated produced appreciable amounts of TNF, IL-1α, G-CSF and KC (Figure 3A–D). In line with our hypothesis that IL-1α is the apical cytokine, production of TNF as well as G-CSF and KC following microabrasion injury was dependent on IL-1α (Figure 3A, C and D). However, the production of IL-1α as well as G-CSF and KC in microabrated footpads of *Tnf*$^{-/-}$mice was similar to those of WT mice (Figure 3B–D). These data altogether demonstrate IL-1α as the apical cytokine that instigates the inflammatory cascade in the footpads.

To further examine whether TNF plays a pathogenic role in *Ptpn6*^{spin}-mediated skin disease, we generated *Ptpn6*^{spin}× *Il1a*$^{-/-}$, *Ptpn6*^{spin} × *Il1r1*$^{-/-}$, *Ptpn6*^{spin} × *Myd88*$^{-/-}$ and *Ptpn6*^{spin}× *Tnf*$^{-/-}$ mice. As expected, *Ptpn6*^{spin}× *Il1a*$^{-/-}$, *Ptpn6*^{spin} × *Il1r1*$^{-/-}$ and *Ptpn6*^{spin} × *Myd88*$^{-/-}$ mice generated in our facility showed complete protection and were disease free until the end of the experiment, whereas 100% of *Ptpn6*^{spin} mice developed footpad inflammation by day 90 (Figure 3E and Figure S1). *Ptpn6*^{spin} × *Tnf*$^{-/-}$ mice demonstrated significantly delayed disease progression than did *Ptpn6*^{spin} mice, and approximately 50% of the *Ptpn6*^{spin} × *Tnf*$^{-/-}$ mice remained completely protected (Figure 3E). TNF engages adaptor molecule TRADD to induce its downstream signaling events. In line with the disease incidence in *Ptpn6*^{spin} × *Tnf*$^{-/-}$ mice, *Ptpn6*^{spin} × *Trad*$^{-/-}$ mice showed significantly delayed disease development compared to *Ptpn6*^{spin} mice (Figure 3F). Further, approximately 50% of the *Ptpn6*^{spin} × *Trad*$^{-/-}$ mice also remained completely disease free (Figure 3F). Taken together, these results are consistent with the hypothesis that IL-1α acts as an apical cytokine that promotes subsequent production of TNF and other pro-inflammatory cytokines

(G-CSF, KC) that ultimately recruit myeloid cells to drive the autoinflammatory skin disease in *Ptpn6*^{spin} mice (Figure 3A–F). It is important to note that while the protection with IL-1α-deficiency was complete, deletion of the TNF-signaling pathway components only provided partial protection. Given that G-CSF has also been shown to be involved in the progression of disease (Croker et al., 2011), it is possible that TNF, G-CSF and other cytokines and chemokines have redundant roles downstream of IL-1α.

Inflammation in *Ptpn6*^{spin} mice is independent of ITGB3, TLR(2-3-4-7-9), TRIF, NOD2-RIPK2, STING and IFNAR signaling axes

To identify additional accessory molecules upstream of IL-1α that are involved in promoting inflammation in *Ptpn6*^{spin} mice, we systematically analyzed several signaling pathways that regulate IL-1α. Integrin signaling pathways have been proposed to be involved in IL-1α regulation (Di Paolo et al., 2009). However, *Ptpn6*^{spin} × *Itgb3*$^{-/-}$ mice displayed disease progression similar to that of *Ptpn6*^{spin} mice (Figure S3A). TRIF is an important adaptor relaying Toll-like receptor (TLR)3 and TLR4 signaling, which can induce IL-1α production. However, we found *Ptpn6*^{spin} × *Trif*$^{-/-}$ mice developed disease comparable to that of *Ptpn6*^{spin} mice, indicating that TLR3 signaling and the MyD88-independent TLR4 signaling axis were dispensable for disease progression (Figure S3B). We next generated *Ptpn6*^{spin} × *Tlr2*$^{-/-}$, *Ptpn6*^{spin} × *Tlr4*$^{-/-}$, and *Ptpn6*^{spin} × *Tlr2*$^{-/-}$ × *Tlr4*$^{-/-}$ mice to investigate the putative roles of TLR2 and TLR4 in *Ptpn6*^{spin}-associated skin inflammation. Neither single nor combined deletion of TLR2 and TLR4 rescued disease progression in *Ptpn6*^{spin} mice (Figure 3G). Moreover, *Ptpn6*^{spin} mice deficient in TLR3, TLR7 and TLR9 also developed disease at a similar rate when compared to *Ptpn6*^{spin} mice (Figure 3H).

Given these results, we hypothesized that other NF-κB– and ERK-activating mechanisms may contribute to *Ptpn6*^{spin}-induced inflammatory disease (Lukens et al., 2013). NOD1- and NOD2-induced NF-κB and ERK signaling are mediated by RIPK2 (Inohara et al., 2000; Ogura et al., 2001), a protein kinase that is closely related to RIPK1. To determine whether NOD1 and/or NOD2 signaling contributed to disease progression in *Ptpn6*^{spin} mice, we generated *Ptpn6*^{spin} mice that were deficient in NOD2 or RIPK2. However, both *Ptpn6*^{spin} × *Nod2*$^{-/-}$ and *Ptpn6*^{spin} × *Ripk2*$^{-/-}$ mice developed disease (Figure S3C).

Because type I interferon (IFN) signatures are a hallmark of autoimmune diseases and play a critical role in driving disease pathogenesis (Banchereau and Pascual, 2006), we generated *Ptpn6*^{spin} mice that were deficient in IRF3 (a proximal regulator of IFN signaling) or the IFN receptor IFNAR2. Both *Ptpn6*^{spin} × *Irf3*$^{-/-}$ and *Ptpn6*^{spin} × *Ifnar2*$^{-/-}$ mice developed disease, although the disease induction in *Ptpn6*^{spin} × *Ifnar2*$^{-/-}$ mice was delayed compared to that of *Ptpn6*^{spin} mice (Figure 3I). STING (encoded by *Tmem173* gene) is a central adapter for DNA sensors, and autoimmune disease associated with defects in DNA processing can be rescued by STING-deficiency (Cai et al., 2014). STING-deficiency, however, did not block the progression of footpad inflammation in *Ptpn6*^{spin} mice (Figure 3J).

Disease observed in *Ptpn6*^{spin} mice is independent of inflammasome, caspase-1 and pyroptotic cell death (Lukens et al., 2013). However, we recently showed that caspase-1 and caspase-8 play redundant roles in *Pstpip2*^{cmo}-mediated autoimmune osteomyelitis (Gurung

et al., 2016; Lukens et al., 2014). Contrastingly, caspase-1 and caspase-8 deficiency together did not provide protection from *Ptpn6*^{spin}-mediated disease (Figure S3D).

Altogether, these results demonstrate that TLR2, TLR3, TLR4, TLR7, TLR9, TRIF, NOD1, NOD2, RIPK2, type I IFN, STING, Integrin-signaling axes, caspase-1 and caspase-8 are all dispensable for *Ptpn6*^{spin}-mediated footpad inflammation.

RIPK1 scaffolding function provokes disease in *Ptpn6*^{spin} mice

Increased IL-1α expression following microabrasion injury of footpads can be rescued by Nec1 treatment, a pharmacological inhibitor of RIPK1 (Lukens et al., 2013). However, studying the genetic contribution of RIPK1 in *Ptpn6*^{spin}-associated disease had been hampered by perinatal lethality associated with RIPK1-deficient mice (Kelliher et al., 1998). Recent reports have shown that perinatal death of *Ripk1*$^{-/-}$ mice can be rescued by deleting both RIPK3 and caspase-8 (i.e., *Casp8*$^{-/-}$ × *Ripk3*$^{-/-}$ × *Ripk1*$^{-/-}$ mice are normal at birth and survive perinatal death) (Dillon et al., 2014; Kaiser et al., 2014; Rickard et al., 2014). To investigate whether germline deletion of RIPK1 rescues disease in *Ptpn6*^{spin} mice, we generated *Ptpn6*^{spin} × *Casp8*$^{-/-}$ × *Ripk3*$^{-/-}$ × *Ripk1*$^{-/-}$ mice (Figure 4A). Although all *Ptpn6*^{spin}, *Ptpn6*^{spin} × *Ripk3*$^{-/-}$, and *Ptpn6*^{spin} × *Casp8*$^{-/-}$ × *Ripk3*$^{-/-}$ mice developed footpad inflammation, *Ptpn6*^{spin} × *Casp8*$^{-/-}$ × *Ripk3*$^{-/-}$ × *Ripk1*$^{-/-}$ mice were significantly protected (Figure 4A and B). Neutrophilia and serum G-CSF and KC cytokines, which are indicators of disease in *Ptpn6*^{spin} mice, were also substantially reduced in *Ptpn6*^{spin} × *Casp8*$^{-/-}$ × *Ripk3*$^{-/-}$ × *Ripk1*$^{-/-}$ mice (Figure S3E). In agreement with results from recently reported fetal liver chimera studies (Lukens et al., 2013), our results confirmed a critical role for RIPK1 in controlling *Ptpn6*^{spin}-mediated skin disease.

RIPK1 has several important functions that can act independently to affect cellular functions (Weinlich and Green, 2014). RIPK1 can phosphorylate target proteins, promote necroptosis (in combination with RIPK3), or act as a scaffold protein. K45A and D148N mutations in RIPK1 eliminate its kinase activity (Berger et al., 2014; Polykratis et al., 2014). To determine whether RIPK1 kinase activity is required for autoinflammation in *Ptpn6*^{spin} mice, *Ptpn6*^{spin} × *Ripk1*^{K45A} mice were generated (Figure 4C). *Ptpn6*^{spin} × *Ripk1*^{K45A} mice developed disease, and histological lesions similar to that of *Ptpn6*^{spin} mice (Figure 4C and D). Although we previously ruled out a role for RIPK3 in skin inflammation (Figure 4A) (Lukens et al., 2013), we hypothesized that RIPK1 might coordinate necroptosis by activating mixed lineage kinase domain-like (MLKL) in a RIPK3-independent fashion. MLKL is an obligate pseudokinase that promotes necroptosis by facilitating pore formation in the plasma membrane (Dondelinger et al., 2014). Nonetheless, *Ptpn6*^{spin}× *Mlkl*$^{-/-}$ mice developed disease and histological lesions with similar kinetics as those of *Ptpn6*^{spin} mice (Figure 4E and F). These results demonstrate that RIPK1 kinase activity and MLKL-induced necroptosis are dispensable for disease progression and implicate RIPK1 scaffolding function in the autoinflammatory skin disease observed in *Ptpn6*^{spin} mice.

TAK1 signaling in myeloid cells is critical for disease progression in *Ptpn6*^{spin} mice

Ubiquitinated RIPK1 acts as a scaffold to support TAK1 recruitment to the RIPK1 complex (Lee et al., 2004). Furthermore, TAK1 is central to signaling events downstream of IL-1R

and TLRs (Ajibade et al., 2013). On the basis that RIPK1 scaffolding function is required for disease progression (Figure 4A–F), we postulated that TAK1 may be involved downstream of RIPK1 to promote disease in *Ptpn6*^{spin} mice. Because TAK1-deficiency is embryonically lethal in mice (Sato et al., 2005; Shim et al., 2005), we bred *Tak1*$^{fl/fl}$ and *Lyz2*$^{cre+}$ mice to generate mice with myeloid-specific deletion of TAK1. Compared to *Ptpn6*^{spin} mice, *Ptpn6*^{spin} × *Tak1*$^{fl/fl}$ × *Lyz2*$^{cre+}$ mice had markedly limited disease progression (Figure 4G and H), identifying TAK1 as a central regulator of inflammation and disease progression in *Ptpn6*^{spin} mice. Hence, RIPK1's scaffolding function and TAK1 are centrally required to modulate inflammation.

MyD88 is critical in both hematopoietic and non-hematopoietic compartments for disease progression in *Ptpn6*^{spin} mice

While we have shown specific roles for IL-1α, TNF and RIPK1-TAK1 signaling axis in promoting skin inflammation in *Ptpn6*^{spin} mice (Figure 1–4), the molecular targets of SHP1 and how SHP1 regulates inflammation are not known. SHP1 is a tyrosine phosphatase that dephosphorylates target proteins to exert its function (Zhang et al., 2000). Previous studies have shown that SHP1 regulates cell survival, proliferation, migration, and inflammation through the control of major signaling pathways that include AKT, JAK-STAT, MAPK, and NFκB (Chong and Maiese, 2007). In line with previous studies (Croker et al., 2008), our data presented here demonstrated a critical role for MyD88 in promoting inflammation in *Ptpn6*^{spin} mice (Figure S1B). To determine whether MyD88 is required in the hematopoietic or radioresistant compartment, we generated *Ptpn6*^{spin} ≫ *Myd88*$^{-/-}$ and *Ptpn6*^{spin} × *Myd88*$^{-/-}$ ≫ WT chimeras, respectively. *Ptpn6*^{spin} ≫ *Myd88*$^{-/-}$ mice were completely protected, as demonstrated by the disease incidence and histologic lesions (Figure 5A and B). MyD88 was also required in the hematopoietic compartment, as *Ptpn6*^{spin} × *Myd88*$^{-/-}$ ≫ WT mice had significantly fewer disease incidence than *Ptpn6*^{spin} ≫ WT chimeras (Figure 5C and D). Altogether, these studies show that MyD88 signaling is required in both hematopoietic and radioresistant compartments to promote inflammatory skin disease in *Ptpn6*^{spin} mice.

SHP1 interacts with MyD88 and regulates phosphorylation of MyD88 tyrosine residues

Given that the *Ptpn6*^{spin} mutation in hematopoietic cells is critical for disease induction (Figure 1), we hypothesized that SHP1-dependent regulation of tyrosine phosphorylation may likely be affected in myeloid cells. To address to what extent global tyrosine phosphorylation were altered in *Ptpn6*^{spin} myeloid cells, we analyzed cell lysates of IL-1α-stimulated WT and *Ptpn6*^{spin} myeloid cells by immunoblotting using the pTyr antibody 4G10. Although we did not detect a global increase in tyrosine phosphorylation in *Ptpn6*^{spin} cell lysates, selected proteins were found hyperphosphorylated following IL-1α stimulation when compared to WT cell lysates, consistent with specificity to SHP1 function (Figure 5E). Considering that MyD88 is critical for regulating NFκB and MAPK signaling pathways downstream of IL-1R, we co-immunoprecipitated tyrosine phosphorylated proteins with pTyr (4G10) antibodies and probed the co- immunoprecipitated lysates for MyD88. IL-1α treatment of WT myeloid cells resulted in a decrease in MyD88 tyrosine phosphorylation. In contrast, MyD88 remained stably phosphorylated following IL-1α stimulation of SHP1-deficient cells (Figure 5F, left panel). Similar to primary cells, MyD88 expressed in HEK

293 C6 cells (IL-1R1 stably expressed) was also tyrosine phosphorylated following IL-1α stimulation (Figure 5F, right panel). These findings show that 1) MyD88 is phosphorylated on tyrosine residues and 2) the SPIN mutation, which attenuates SHP1 function, leads to sustained elevated tyrosine phosphorylation of MyD88 during IL-1α stimulation.

SHP1 contains Src homology 2 (SH2) domain that it utilizes to bind to phosphorylated tyrosine residues on target proteins (Chong and Maiese, 2007). In fact, the SPIN mutation, Y208N, alters a residue in the sequence linking the two SH2 domains. We examined whether SHP1 interacted with MyD88 by overexpressing both SHP1 and MyD88 in HEK 293 C6 cells. Our results demonstrated that, following IL-1α stimulation, SHP1 interacted with MyD88 (Figure 5G, upper panel). Furthermore, the substrate-trapping mutant form of SHP1 (SHP1 DA) and the functionally attenuated SHP1 from *Ptpn6*^{spin} mice (SHP1 Y208N) interacted with MyD88 similar to WT SHP1 (Figure 5G). Additionally, mutating a predicted MyD88 tyrosine residue at 116 to phenylalanine [this tyrosine residue is absent in alternatively spliced MyD88 (MyD88s), which act as a negative regulator of IL-1R signaling (Burns et al., 2003)] did not prevent SHP1 interaction with MyD88 (Figure 5G). The interactions between SHP1 and MyD88 were specific because similarly overexpressed SHP2 did not interact with MyD88 (Figure 5G, lower panel). These data demonstrate a previously uncharacterized role for SHP1 in regulating MyD88 phosphorylation and suggest a potential role for this event in preventing autoinflammatory skin disease.

SYK phosphorylates MyD88, and SHP1 inhibits SYK activation to regulate MyD88 phosphorylation

To further delineate the molecular mechanisms involved in tyrosine phosphorylation of MyD88, we investigated potential tyrosine kinases that could phosphorylate MyD88. Our study showed that SYK, but not Breast tumor kinase (BRK) or Bruton's tyrosine kinase (BTK) was able to specifically phosphorylate MyD88 (Figure 6A). We next examined the tyrosine residues on MyD88 that were phosphorylated by SYK by co-transfecting WT or mutant MyD88 along with SYK in HEK293 cells. Our data suggest that tyrosine residues 180 and 278 are two potential sites on MyD88 phosphorylated by SYK (Figure 6B and Figure S4A). We also observed that mutating Y71 residue resulted in increased phosphorylation of MyD88. Phosphorylation of Y71 may act in a self-regulatory negative feedback loop to inhibit additional tyrosine phosphorylation of MyD88. One possible mechanism could be that Y71 phosphorylation recruits additional proteins to halt MyD88 phosphorylation. Whether increased MyD88 phosphorylation observed in Y71F mutants have any functional consequence is not clear and will need further investigation.

It can be posited that SHP1 could directly regulate MyD88 phosphorylation (through its phosphatase activity), or indirectly regulate MyD88 phosphorylation by regulating SYK activation (SYK phosphorylates MyD88- Figure 6A). To test whether SHP1 directly regulates MyD88 phosphorylation, we performed an in vitro dephosphorylation assay where phosphorylated MyD88 was mixed with WT or Y208N mutant SHP1 (Figure S4B). Both WT and mutant SHP1 were unable to dephosphorylate MyD88 suggesting SHP1 does not regulate MyD88 phosphorylation directly (Figure S4B). Expression of SYK and MyD88 in HEK293 C6 cells resulted in SYK-dependent MyD88 phosphorylation, which is

dephosphorylated by WT SHP1, but to a lesser extent by Y208N or DA mutant SHP1 (Figure 6C). In these studies, WT SHP1 but not Y208N or DA mutant SHP1 reduced phosphorylation of SYK suggesting a role for SHP1 in inhibiting SYK phosphorylation, which could be a possible mechanism for MyD88 dephosphorylation (Figure 6C). To determine whether SHP1 directly regulated SYK activation, SYK was co-expressed with either WT or mutant (Y208 or DA) SHP1. While WT SHP1 co-expression reduced SYK phosphorylation, Y208N or DA SHP1 was less efficient at dephosphorylating SYK (Figure 6D). In line with our hypothesis that SYK regulates IL-1 induced MyD88 signaling, IL-1α-induced NFκB and ERK activation were blunted in the SYK-deficient myeloid cells (Figure S5). These data altogether uncover a previously uncharacterized signaling pathway in which SYK phosphorylates MyD88 and where SHP1 directly regulates SYK activation. Whether SYK is a global regulator of MyD88 signaling is not fully understood and will require further investigation.

SYK deficiency in *Ptpn6*^{spin} mice inhibits inflammatory disease

Given our in vitro data demonstrating a role for SYK in promoting MyD88 phosphorylation, we hypothesized that SYK deletion in *Ptpn6*^{spin} mice would rescue the autoinflammatory skin disease. Since SYK-deficient mice die perinatally (Cheng et al., 1995), we bred *Ptpn6*^{spin} mice with *Syk*$^{fl/fl}$ × *Lyz2*$^{cre+}$ mice to test the functional relevance of SYK in disease progression in *Ptpn6*^{spin} mice. Consistent with the in vitro data demonstrating an important role for SYK in phosphorylating MyD88, *Ptpn6*^{spin} × *Syk*$^{fl/fl}$ × *Lyz2*$^{cre+}$ mice were protected from disease induction and histologic lesions (Figure 6E and F). Thus, conditional deletion of SYK specifically in the myeloid cells is sufficient to provide protection from skin inflammation observed in the *Ptpn6*^{spin} mice.

DISCUSSION

Polymorphisms in the human *FTFN6* gene are associated with a wide spectrum of autoinflammatory diseases (Cao and Hegele, 2002; Christophi et al., 2008). Therefore, understanding the basic biology and molecular mechanisms of these inflammatory disorders is crucial for developing improved treatment options. Using *Ptpn6*^{spin} and myeloid-specific SHP1-deficient *(Ptpn6*$^{fl/fl}$ × *Lyz2*$^{cre+}$) mouse models, we have discovered several critical checkpoints and complex crosstalk between myeloid and radioresistant cells that are crucial in driving this inflammatory disease.

We undertook a genetic approach to define the molecular mechanisms and signaling pathways that are regulated by SHP1 to modulate inflammation. We demonstrated a central role for IL-1α, IL-1R, MyD88, SYK, RIPK1 and TAK1 in promoting inflammatory disease in *Ptpn6*^{spin} mice (mice with reduced SHP1 phosphatase activity). Importantly, in addition to demonstrating a central role for these molecules in the IL-1R signaling pathway, we also excluded the role of several other signaling pathways. Our studies showed that disease in *Ptpn6*^{spin} mice is independent of IFNAR-signaling, STING (involved in DNA sensing pathway), ITGB3 (Integrin) and NOD2-RIPK2 signaling axis. These studies, although negative, are critical in reinforcing the specific role of IL-1α signaling axis in provoking inflammatory disease in *Ptpn6*^{spin} mice.

RIPK1-deficient mice suffer from perinatal death making it difficult to study the role of this molecule in *Ptpn6*^{spin}-mediated inflammatory disease (Kelliher et al., 1998). To circumvent this perinatal lethality, *Ptpn6*^{spin} × *Ripk1*$^{-/-}$ fetal liver chimeras were generated, which were protected from disease (Lukens et al., 2013). Recent studies have shown that *Ripk1*$^{-/-}$ cells undergo cell death and thus it could be implied that the protection observed in *Ptpn6*^{spin} × *Ripk1*$^{-/-}$ fetal liver chimeras could be due to the gradual loss of these RIPK1-deficient *Ptpn6*^{spin} cells. Therefore to further ascertain the role of RIPK1 in this inflammatory skin disease we took advantage of *Casp8*$^{-/-}$ × *Ripk3*$^{-/-}$ × *Ripk1*$^{-/-}$ mice, which were crossed with *Ptpn6*^{spin} mice (Dillon et al., 2014; Kaiser et al., 2014; Rickard et al., 2014). *Ptpn6*^{spin} × *Casp8*$^{-/-}$ × *Ripk3*$^{-/-}$ × *Ripk1*$^{-/-}$ mice showed significant protection from footpad inflammation and disease progression. Surprisingly, about 10 percent of *Ptpn6*^{spin} × *Casp8*$^{-/-}$ × *Ripk3*$^{-/-}$ × *Ripk1*$^{-/-}$ mice still developed footpad inflammation with delayed kinetics, which we have speculated to be a result of age related lymphoproliferative and autoinflammatory disorder associated with *Casp8*$^{-/-}$ × *Ripk3*$^{-/-}$ × *Ripk1*$^{-/-}$ mice (Dillon et al., 2014). Mechanistically, we demonstrated that RIPK1 scaffolding function and TAK1 signaling in myeloid cells are central regulators of footpad inflammation in *Ptpn6*^{spin} mice. However, myeloid specific deletion of *Tak1* in *Ptpn6*^{spin} mice still induced disease in about 15–20 percent of the mice. We propose the leaky *Lyz2*^{cre} induced deletion of *Tak1* in myeloid cells and autoimmunity associated with aged *Tak1*$^{fl/fl}$ × *Lyz2*$^{cre+}$ mice for the 15–20% disease observed in otherwise protected *Ptpn6*^{spin} × *Tak1*$^{fl/fl}$ × *Lyz2*$^{cre+}$ mice (Ajibade et al., 2012; Elefteriou and Yang, 2011; Lamothe et al., 2012).

MyD88 is a central adaptor molecule for TLRs and IL-1R, and induce activation of several critical signaling pathways. The importance of MyD88 in pathogen sensing has been well established in the field as demonstrated by the heightened susceptibility of *Myd88*$^{-/-}$ mice to variety of infections. As demonstrated by our group and others, MyD88 plays an essential role in inflammatory disease in *Ptpn6*^{spin} mice (Croker et al., 2008). Here, we further demonstrated that MyD88 was required in both hematopoietic and radioresistant compartments to provoke disease in *Ptpn6*^{spin} mice. The requirement of MyD88 in the *Ptpn6*^{spin} myeloid cells was so that they could respond to IL-1α cytokines that were released by the radioresistant cells. Why MyD88 is required in the radioresistant compartment is not clear; however, we can envision at least two scenarios that may potentially explain the requirement for MyD88 in the radioresistant compartment. One, IL-1R is required in the radioresistant compartment (i.e. *Ptpn6*^{spin} ≫ *Il1r1*$^{-/-}$ mice are protected- Figure 2C) and thus IL-1α released by the radioresistant cells may act in a positive feedback loop through IL-1R-MyD88 signaling in the radioresistant compartment to amplify cytokine response and to recruit the disease instigating *Ptpn6*^{spin} myeloid cells. Second, MyD88 could be required for microbiota-induced IL-1α expression. This second possibility is supported by our studies and a published study (Croker et al., 2008), which both demonstrate that the microbiome is required for disease development in *Ptpn6*^{spin} mice. These hypotheses are supported by studies that show that *Ptpn6*^{spin} mice derived in germ-free facilities do not develop the inflammatory disease (Croker et al., 2008).

Although the molecular mechanisms involved in the MyD88 signaling have been thoroughly explored; how posttranslational modifications of MyD88 affects it's signaling activity has been severely understudied (Deguine and Barton, 2014). Herein, we report that MyD88 is

posttranslationally modified via its tyrosine residue phosphorylation. More importantly, we have also identified SYK as the kinase that phosphorylates MyD88. Additional studies are needed to study the functional consequence of these posttranslational modifications on MyD88 and how they impact the inflammatory disease in *Ptpn6*^{spin} mice.

In conclusion, we have shown that IL-1α is an apical cytokine that regulates production of TNF, G-CSF and KC to drive inflammatory disease observed in *Ptpn6*^{spin} mice. We have demonstrated that RIPK1 scaffolding function and TAK1-mediated signaling in myeloid cells are central regulators of footpad inflammation in *Ptpn6*^{spin} mice. We further revealed that MyD88 play critical roles in both the hematopoietic and stromal compartments in *Ptpn6*^{spin}-mediated disease. We also demonstrated that SYK is a critical tyrosine kinase that promotes MyD88 phosphorylation and provokes disease in *Ptpn6*^{spin} mice. Our studies revealed that attenuation of SHP1 by a SPIN mutation is associated with elevated MyD88 phosphorylation during IL-1α signaling events. Finally, we showed that SHP1 controls SYK activation to regulate MyD88 phosphorylation. Our results have uncovered several important cellular and molecular checkpoints that are required for potentiation of inflammation in the absence of functional SHP1. IL-1α-neutralizing approaches as well as targeting RIPK1-TAK1 signaling axis or SYK and MyD88 phosphorylation may be effective therapeutic strategies to treat inflammatory skin disorders.

EXPERIMENTAL PROCEDURES

Mice

Genetic mutant mice were previously described or were purchased from the Jackson laboratory (please see supplemental procedures for details). All mice were kept in specific pathogen-free conditions within the Animal Resource Center at St. Jude Children's Research Hospital. Animal studies were conducted by using protocols approved by the Institutional Animal Care and Use Committee of St. Jude Children's Research Hospital.

Histopathology

Formalin-preserved feet were processed and embedded in paraffin according to standard procedures. Sections (5-μm thick) were stained with hematoxylin and eosin (H&E), and images were acquired using light microscopy.

Microabrasion injury model

WT, *Il1a*$^{-/-}$, and *Tnf*$^{-/-}$ mice were anesthetized in Isoflurane chambers, and the plantar surfaces of hind paws were irritated to induce physical trauma by gently rubbing with sterile sandpaper 10 times. Mice were euthanized 6 hours post microabrasion, and footpads were analyzed for protein expression of IL-1α, TNF, G-CSF, and KC by performing ELISAs.

ELISA

Cytokine ELISAs were performed according to the manufacturer's instructions (Milliplex).

Flow cytometry protocols and antibodies

CD11b (M1/70), and Gr-1 (RB6-8C5) antibodies from eBioscience were used for flow cytometry. Flow cytometry data were acquired on an upgraded eight-color FACScan and analyzed by using FlowJo software (Tree Star).

Bone marrow chimeras

Bone marrow was flushed from the femurs and filtered through a 40-μm filter. A total of 3×10^6–5×10^6 cells in 200 μL PBS were transferred into lethally irradiated (1,000 rad) mice via retroorbital sinus injection.

Plasmids, site-directed mutagenesis, and transfection

The following mammalian expression plasmids were purchased from Addgene: MyD88-FLAG (#13093), HA-MyD88 (#12287); SYK (#20646), BTK (#20432) and pJ3-SHP1 (#8572). Other plasmid used in this study: pcDNA3.1-HA-SHP2 and pLPC-BRK.

Agilent's manufacturer protocol was followed to perform site-directed mutagenesis. The following primers were used: SHP1 D419A trapping mutation (Fwd: gtacctgagctggcccgCccatggggtcccc, Rev: ggggaccccatggGcgggccagctcaggtac); SHP1 Y208N Spin mutation (Fwd: ggcgcctttgtcAacctgcggcagccgtac; Rev: gtacggctgccgcaggtTgacaaaggcgcc); SHP2 D425A trapping mutation (Fwd: cggacctggccggCccacggcgtgcccagc; Rev: gctgggcacgccgtggGccggccaggtccg); MyD88 (mouse) Y116F mutation (Fwd: ggactgccagaaatTcttaggtaagcagcag; Rev: ctgctgcttacctaagAatttctggcagtcc); MyD88 (human) Y71F mutation (Fwd: ggagatggactttgagtTcttggagatccggc; Rev: gccggatctccaagAactcaaagtccatctcc); MyD88 (human) Y129F mutation (Fwd: ggaggattgccaaaagtTtatcttgaagcagc; Rev: gctgcttcaagataAacttttggcaatcctcc); MyD88 (human) Y180F mutation (Fwd: cgatgccttcatctgctTttgccccagcgac; Rev: gtcgctggggcaaAagcagatgaaggcatcg); MyD88 (human) Y200F mutation (Fwd: ggaacagacaaactTtcgactgaagttgtg; Rev: cacaacttcagtcgaAagtttgtctgttcc); MyD88 (human) Y248F mutation (Fwd: ggttgtctctgatgattTcctgcagagcaagg; Rev: ccttgctctgcaggAaatcatcagagacaacc); MyD88 (human) Y278F mutation (Fwd: gatccccatcaagtTcaaggcaatgaag; Rev: cttcattgccttgAacttgatggggatc); and MyD88 (human) Y297F mutation (Fwd: cactgtctgcgactTcaccaacccctgcacc; Rev: ggtgcaggggttggtgAagtcgcagacagtg).

Mirus' manufacturer protocol was followed to perform transient transfection (Transit-2020, Mirus). In brief, HEK293 or HEK293 IL-1R1 C6 cells (from Geroge Stark, Cleveland Clinic) were seeded in a 6-well plate one day before transfection. Plasmid (2 μg) and Mirus transfection reagent (5 μL) were added to each well's experiment. Whole-cell lysates were collected 24 h after transfection.

Antibodies and immunoprecipitation

The following antibodies were used in the analysis:

From Millipore: phosphor-Tyr(4G10), phosphor-Tyr342 and total BRK; from Cell Signaling: phospho-Tyr525/6 and total SYK, phospho-Tyr223 and total BTK, ERK1/2; from Abcam:

MyD88; from Santa Cruz: SHP1; from Covance: HA; from Sigma: FLAG and ß-actin. Cell extracts were prepared in lysis buffer (20 mM HEPES pH 7.5, 150 mM NaCl, 1% NP-40, and freshly added protease inhibitor cocktail from Roche) and analyzed by performing SDS-PAGE and immunoblotting.

Pre-cleared cell extracts were incubated with the indicated antibody for 4 h on a rotator in a cold room and then incubated 1:1 with Protein A/G agarose beads (GE) for 1h for immunoprecipitation. Immunoprecipates were washed in lysis buffer three times before electrophoresis.

Statistical analysis

All results are presented as means ± standard errors. Disease curves were analyzed by performing Log-rank (Mantel-Cox) testing, and significant differences between two groups were determined by performing Mann-Whitney test. Differences were considered statistically significant when $P<0.05$. *$P<0.05$, **$P<0.01$, ***$P<0.001$.

Supplementary Material

Refer to Web version on PubMed Central for supplementary material.

Acknowledgments

We thank B.A. Buetler, V.M. Dixit, M. Kelliher, and D.R. Green for generously supplying mutant mice. We also thank members of the Kanneganti laboratory for their helpful discussion and reviewing of the manuscript. We thank the Hartwell Center for Bioinformatics and Biotechnology and the Department of Computational Biology at St. Jude for help with Microbiome studies. Images were acquired at the SJCRH Cell & Tissue Imaging Center, which is supported by SJCRH and NCI P30 CA021765-35. This work was supported by the National Institutes of Health Grants CA53840 and GM55989 to N.K.T., and Grants CA163507, AR056296, AI124346 and AI101935 and the American Lebanese Syrian Associated Charities (ALSAC) to T.-D.K.

Abbreviations

NLR	NOD-like receptor
SYK	Spleen tyrosine kinase
RIPK	Receptor interacting protein kinase
Nec-1	necrostatin-1
IL	interleukin
WT	wild-type

References

Abram CL, Roberge GL, Pao LI, Neel BG, Lowell CA. Distinct roles for neutrophils and dendritic cells in inflammation and autoimmunity in motheaten mice. Immunity. 2013; 38:489–501. [PubMed: 23521885]

Ajibade AA, Wang HY, Wang RF. Cell type-specific function of TAK1 in innate immune signaling. Trends in immunology. 2013; 34:307–316. [PubMed: 23664135]

Ajibade AA, Wang Q, Cui J, Zou J, Xia X, Wang M, Tong Y, Hui W, Liu D, Su B, et al. TAK1 negatively regulates NF-kappaB and p38 MAP kinase activation in Gr-1+CD11b+ neutrophils. Immunity. 2012; 36:43–54. [PubMed: 22226633]

Banchereau J, Pascual V. Type I interferon in systemic lupus erythematosus and other autoimmune diseases. Immunity. 2006; 25:383–392. [PubMed: 16979570]

Berger SB, Kasparcova V, Hoffman S, Swift B, Dare L, Schaeffer M, Capriotti C, Cook M, Finger J, Hughes-Earle A, et al. Cutting Edge: RIP1 kinase activity is dispensable for normal development but is a key regulator of inflammation in SHARPIN-deficient mice. J Immunol. 2014; 192:5476–5480. [PubMed: 24821972]

Burns K, Janssens S, Brissoni B, Olivos N, Beyaert R, Tschopp J. Inhibition of interleukin 1 receptor/Toll-like receptor signaling through the alternatively spliced, short form of MyD88 is due to its failure to recruit IRAK-4. The Journal of experimental medicine. 2003; 197:263–268. [PubMed: 12538665]

Cai X, Chiu YH, Chen ZJ. The cGAS-cGAMP-STING pathway of cytosolic DNA sensing and signaling. Molecular cell. 2014; 54:289–296. [PubMed: 24766893]

Cao H, Hegele RA. Identification of polymorphisms in the human SHP1 gene. J Hum Genet. 2002; 47:445–447. [PubMed: 12181644]

Chen CJ, Kono H, Golenbock D, Reed G, Akira S, Rock KL. Identification of a key pathway required for the sterile inflammatory response triggered by dying cells. Nat Med. 2007; 13:851–856. [PubMed: 17572686]

Cheng AM, Rowley B, Pao W, Hayday A, Bolen JB, Pawson T. Syk tyrosine kinase required for mouse viability and B-cell development. Nature. 1995; 378:303–306. [PubMed: 7477353]

Chong ZZ, Maiese K. The Src homology 2 domain tyrosine phosphatases SHP-1 and SHP-2: diversified control of cell growth, inflammation, and injury. Histol Histopathol. 2007; 22:1251–1267. [PubMed: 17647198]

Christophi GP, Hudson CA, Gruber RC, Christophi CP, Mihai C, Mejico LJ, Jubelt B, Massa PT. SHP-1 deficiency and increased inflammatory gene expression in PBMCs of multiple sclerosis patients. Lab Invest. 2008; 88:243–255. [PubMed: 18209728]

Cohen I, Rider P, Carmi Y, Braiman A, Dotan S, White MR, Voronov E, Martin MU, Dinarello CA, Apte RN. Differential release of chromatin-bound IL-1alpha discriminates between necrotic and apoptotic cell death by the ability to induce sterile inflammation. Proc Natl Acad Sci U S A. 2010; 107:2574–2579. [PubMed: 20133797]

Croker BA, Lawson BR, Rutschmann S, Berger M, Eidenschenk C, Blasius AL, Moresco EM, Sovath S, Cengia L, Shultz LD, et al. Inflammation and autoimmunity caused by a SHP1 mutation depend on IL-1, MyD88, and a microbial trigger. Proc Natl Acad Sci U S A. 2008; 105:15028–15033. [PubMed: 18806225]

Croker BA, Lewis RS, Babon JJ, Mintern JD, Jenne DE, Metcalf D, Zhang JG, Cengia LH, O'Donnell JA, Roberts AW. Neutrophils require SHP1 to regulate IL-1beta production and prevent inflammatory skin disease. J Immunol. 2011; 186:1131–1139. [PubMed: 21160041]

Deguine J, Barton GM. MyD88: a central player in innate immune signaling. F1000Prime Rep. 2014; 6:97. [PubMed: 25580251]

Di Paolo NC, Miao EA, Iwakura Y, Murali-Krishna K, Aderem A, Flavell RA, Papayannopoulou T, Shayakhmetov DM. Virus binding to a plasma membrane receptor triggers interleukin-1 alpha-mediated proinflammatory macrophage response in vivo. Immunity. 2009; 31:110–121. [PubMed: 19576795]

Dillon CP, Weinlich R, Rodriguez DA, Cripps JG, Quarato G, Gurung P, Verbist KC, Brewer TL, Llambi F, Gong YN, et al. RIPK1 blocks early postnatal lethality mediated by caspase-8 and RIPK3. Cell. 2014; 157:1189–1202. [PubMed: 24813850]

Dondelinger Y, Declercq W, Montessuit S, Roelandt R, Goncalves A, Bruggeman I, Hulpiau P, Weber K, Sehon CA, Marquis RW, et al. MLKL compromises plasma membrane integrity by binding to phosphatidylinositol phosphates. Cell reports. 2014; 7:971–981. [PubMed: 24813885]

Elefteriou F, Yang X. Genetic mouse models for bone studies—strengths and limitations. Bone. 2011; 49:1242–1254. [PubMed: 21907838]

Green MC, Shultz LD. Motheaten, an immunodeficient mutant of the mouse. I. Genetics and pathology. J Hered. 1975; 66:250–258. [PubMed: 1184950]

Gurung P, Burton A, Kanneganti TD. NLRP3 inflammasome plays a redundant role with caspase 8 to promote IL-1beta-mediated osteomyelitis. Proc Natl Acad Sci U S A. 2016; 113:4452–4457. [PubMed: 27071119]

Inohara N, Koseki T, Lin J, del Peso L, Lucas PC, Chen FF, Ogura Y, Nunez G. An induced proximity model for NF-kappa B activation in the Nod1/RICK and RIP signaling pathways. J Biol Chem. 2000; 275:27823–27831. [PubMed: 10880512]

Kaiser WJ, Daley-Bauer LP, Thapa RJ, Mandal P, Berger SB, Huang C, Sundararajan A, Guo H, Roback L, Speck SH, et al. RIP1 suppresses innate immune necrotic as well as apoptotic cell death during mammalian parturition. Proc Natl Acad Sci U S A. 2014; 111:7753–7758. [PubMed: 24821786]

Kelliher MA, Grimm S, Ishida Y, Kuo F, Stanger BZ, Leder P. The death domain kinase RIP mediates the TNF-induced NF-kappaB signal. Immunity. 1998; 8:297–303. [PubMed: 9529147]

Lamothe B, Lai Y, Hur L, Orozco NM, Wang J, Campos AD, Xie M, Schneider MD, Lockworth CR, Jakacky J, et al. Deletion of TAK1 in the myeloid lineage results in the spontaneous development of myelomonocytic leukemia in mice. PloS one. 2012; 7:e51228. [PubMed: 23251462]

Lee TH, Shank J, Cusson N, Kelliher MA. The kinase activity of Rip1 is not required for tumor necrosis factor-alpha-induced IkappaB kinase or p38 MAP kinase activation or for the ubiquitination of Rip1 by Traf2. J Biol Chem. 2004; 279:33185–33191. [PubMed: 15175328]

Lukens JR, Gurung P, Vogel P, Johnson GR, Carter RA, McGoldrick DJ, Bandi SR, Calabrese CR, Vande Walle L, Lamkanfi M, et al. Dietary modulation of the microbiome affects autoinflammatory disease. Nature. 2014; 516:246–249. [PubMed: 25274309]

Lukens JR, Vogel P, Johnson GR, Kelliher MA, Iwakura Y, Lamkanfi M, Kanneganti TD. RIP1-driven autoinflammation targets IL-1alpha independently of inflammasomes and RIP3. Nature. 2013; 498:224–227. [PubMed: 23708968]

Martin A, Tsui HW, Tsui FW. SHP-1 variant proteins are absent in motheaten mice despite presence of splice variant transcripts with open reading frames. Molecular immunology. 1999; 36:1029–1041. [PubMed: 10698306]

Naik S, Bouladoux N, Linehan JL, Han SJ, Harrison OJ, Wilhelm C, Conlan S, Himmelfarb S, Byrd AL, Deming C, et al. Commensal-dendritic-cell interaction specifies a unique protective skin immune signature. Nature. 2015; 520:104–108. [PubMed: 25539086]

Naik S, Bouladoux N, Wilhelm C, Molloy MJ, Salcedo R, Kastenmuller W, Deming C, Quinones M, Koo L, Conlan S, et al. Compartmentalized control of skin immunity by resident commensals. Science. 2012; 337:1115–1119. [PubMed: 22837383]

Nesterovitch AB, Szanto S, Gonda A, Bardos T, Kis-Toth K, Adarichev VA, Olasz K, Ghassemi-Najad S, Hoffman MD, Tharp MD, et al. Spontaneous insertion of a b2 element in the ptpn6 gene drives a systemic autoinflammatory disease in mice resembling neutrophilic dermatosis in humans. Am J Pathol. 2011; 178:1701–1714. [PubMed: 21435452]

Ogura Y, Inohara N, Benito A, Chen FF, Yamaoka S, Nunez G. Nod2, a Nod1/Apaf-1 family member that is restricted to monocytes and activates NF-kappaB. J Biol Chem. 2001; 276:4812–4818. [PubMed: 11087742]

Polykratis A, Hermance N, Zelic M, Roderick J, Kim C, Van TM, Lee TH, Chan FK, Pasparakis M, Kelliher MA. Cutting edge: RIPK1 Kinase inactive mice are viable and protected from TNF-induced necroptosis in vivo. J Immunol. 2014; 193:1539–1543. [PubMed: 25015821]

Rickard JA, O'Donnell JA, Evans JM, Lalaoui N, Poh AR, Rogers T, Vince JE, Lawlor KE, Ninnis RL, Anderton H, et al. RIPK1 regulates RIPK3-MLKL-driven systemic inflammation and emergency hematopoiesis. Cell. 2014; 157:1175–1188. [PubMed: 24813849]

Rider P, Carmi Y, Guttman O, Braiman A, Cohen I, Voronov E, White MR, Dinarello CA, Apte RN. IL-1alpha and IL-1beta recruit different myeloid cells and promote different stages of sterile inflammation. J Immunol. 2011; 187:4835–4843. [PubMed: 21930960]

Sato S, Sanjo H, Takeda K, Ninomiya-Tsuji J, Yamamoto M, Kawai T, Matsumoto K, Takeuchi O, Akira S. Essential function for the kinase TAK1 in innate and adaptive immune responses. Nature immunology. 2005; 6:1087–1095. [PubMed: 16186825]

Shim JH, Xiao C, Paschal AE, Bailey ST, Rao P, Hayden MS, Lee KY, Bussey C, Steckel M, Tanaka N, et al. TAK1, but not TAB1 or TAB2, plays an essential role in multiple signaling pathways in vivo. Genes & development. 2005; 19:2668–2681. [PubMed: 16260493]

Shultz LD, Coman DR, Bailey CL, Beamer WG, Sidman CL. "Viable motheaten," a new allele at the motheaten locus. I. Pathology. Am J Pathol. 1984; 116:179–192. [PubMed: 6380298]

Shultz LD, Schweitzer PA, Rajan TV, Yi T, Ihle JN, Matthews RJ, Thomas ML, Beier DR. Mutations at the murine motheaten locus are within the hematopoietic cell protein-tyrosine phosphatase (Hcph) gene. Cell. 1993; 73:1445–1454. [PubMed: 8324828]

Tsui HW, Siminovitch KA, de Souza L, Tsui FW. Motheaten and viable motheaten mice have mutations in the haematopoietic cell phosphatase gene. Nat Genet. 1993; 4:124–129. [PubMed: 8348149]

Weinlich R, Green DR. The two faces of receptor interacting protein kinase-1. Molecular cell. 2014; 56:469–480. [PubMed: 25459879]

Wishcamper CA, Coffin JD, Lurie DI. Lack of the protein tyrosine phosphatase SHP-1 results in decreased numbers of glia within the motheaten (me/me) mouse brain. The Journal of comparative neurology. 2001; 441:118–133. [PubMed: 11745639]

Zhang J, Somani AK, Siminovitch KA. Roles of the SHP-1 tyrosine phosphatase in the negative regulation of cell signalling. Semin Immunol. 2000; 12:361–378. [PubMed: 10995583]

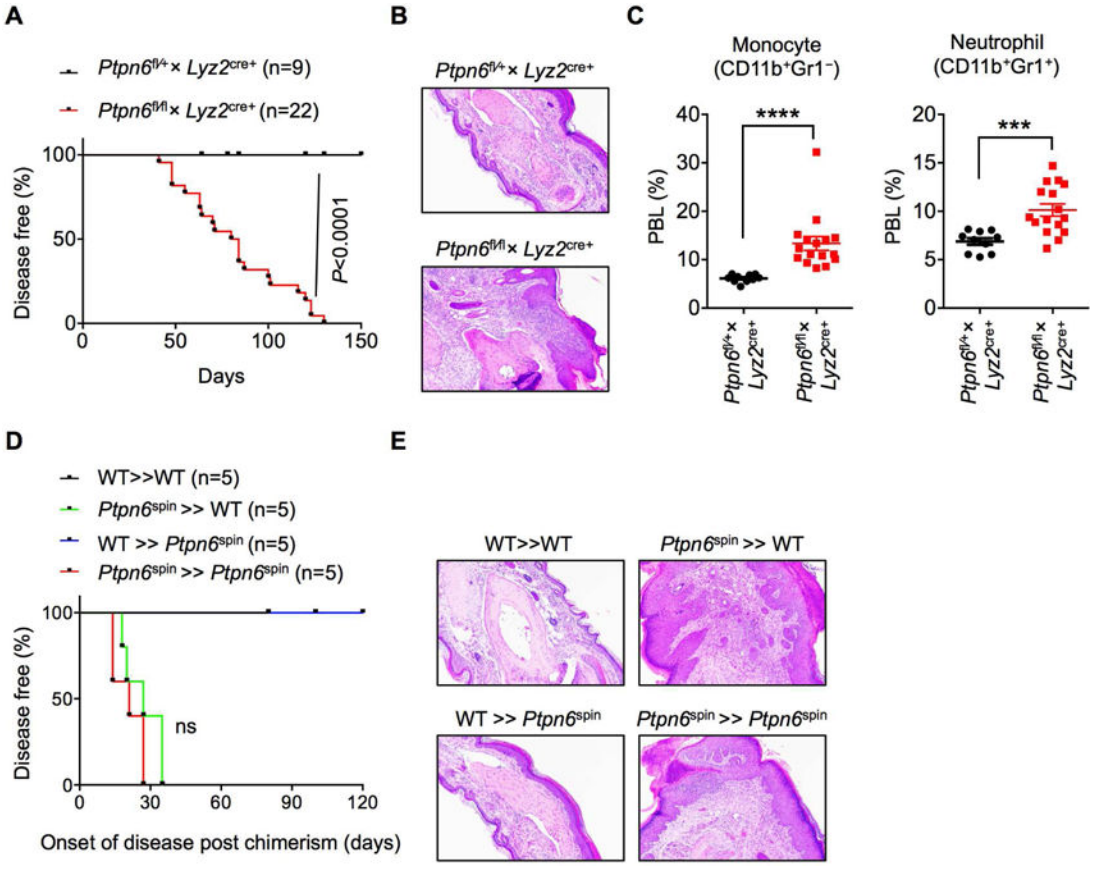

Figure 1. *Ptpn6* mutation or deletion in the myeloid cells is critical for driving autoinflammatory skin disease. Please see also Table S1

(**A–C**) *Ptpn6*$^{fl/fl}$ mice were bred with *Lyz2*$^{cre+}$ mice to generate mice with myeloid specific deficiency of *Ptpn6.* Disease curve (**A**), and H&E stain (**B**) in *Ptpn6*$^{fl/fl}$ × *Lyz2*$^{cre+}$ mice compared to littermate control *(Ptpn6*$^{fl/+}$ × *Lyz2*$^{cre+}$*)* mice. **C**, PBL from *Ptpn6*$^{fl/fl}$ × *Lyz2*$^{cre+}$ and littermate controls were analyzed for monocyte and neutrophil population by flow cytometry. **(D–E)** Bone marrow chimeras were generated from WT and *Ptpn6*^{spin} mice. Disease curve **(D)** and H&E stain **(E)** in WT ≫ WT, *Ptpn6*^{spin} ≫ WT, *Ptpn6*^{spin} ≫ *Ptpn6*^{spin} and WT ≫ *Ptpn6*^{spin} chimeras. ns=not significant.

Disease curve in **A and D** was analyzed by Log-rank (Mantel-Cox) test. All data are presented as mean ± s.e.m. Each point represents single mouse and Mann-Whitney test was used to determine significance between the two groups analyzed (**C**). ***P<0.001 ****P<0.0001.

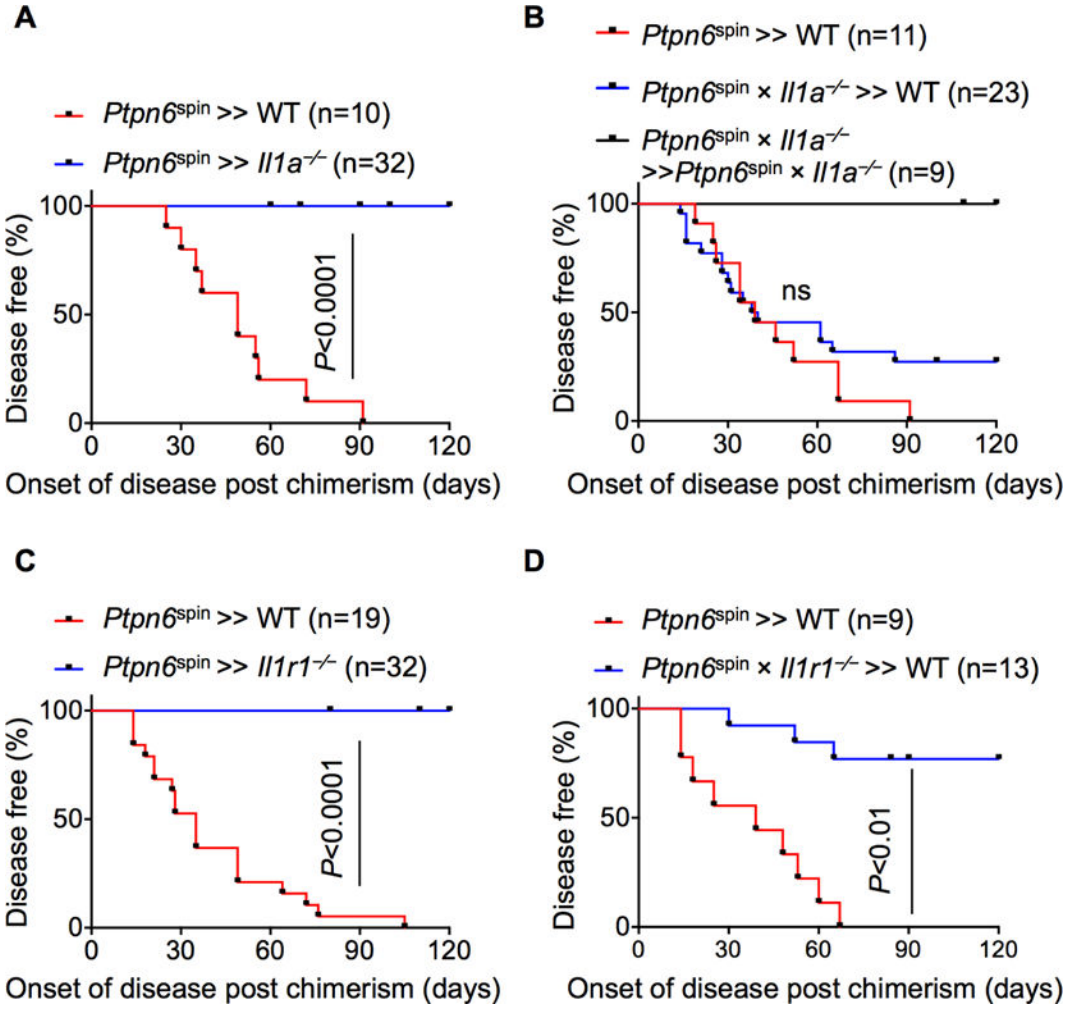

Figure 2. Radioresistant IL-1α signaling through IL-1R in both the radioresistant and hematopoietic compartments instigates inflammatory disease in *Ptpn6*^{spin} mice. Please see also Figure S1 and S2

(A) *Ptpn6*^{spin} bone marrow cells were adoptively transferred into lethally irradiated WT or *Il1a*$^{-/-}$ mice to generate *Ptpn6*^{spin} ≫ WT and *Ptpn6*^{spin} ≫ *Il1a*$^{-/-}$ chimeras and monitored for disease progression.

(B) *Ptpn6*^{spin} ≫ WT, *Ptpn6*^{spin} × *Il1a*$^{-/-}$ ≫ WT and *Ptpn6*^{spin} × *Il1a*$^{-/-}$ ≫ *Ptpn6*^{spin} × *Il1a*$^{-/-}$ chimeras were generated as in **A** and followed for disease progression. ns=not significant denotes comparison between *Ptpn6*^{spin} × *Il1a*$^{-/-}$ ≫ WT and *Ptpn6*^{spin} × *Il1a*$^{-/-}$ ≫ *Ptpn6*^{spin} × *Il1a*$^{-/-}$ chimeras.

(C–D) *Ptpn6*^{spin} ≫ WT, *Ptpn6*^{spin} ≫ *Il1r1*$^{-/-}$ and *Ptpn6*^{spin} × *Il1r1*$^{-/-}$ ≫ WT chimeras were generated as in **A** and followed for disease progression.

Disease curve was analyzed by Log-rank (Mantel-Cox) test. ns=not significant.

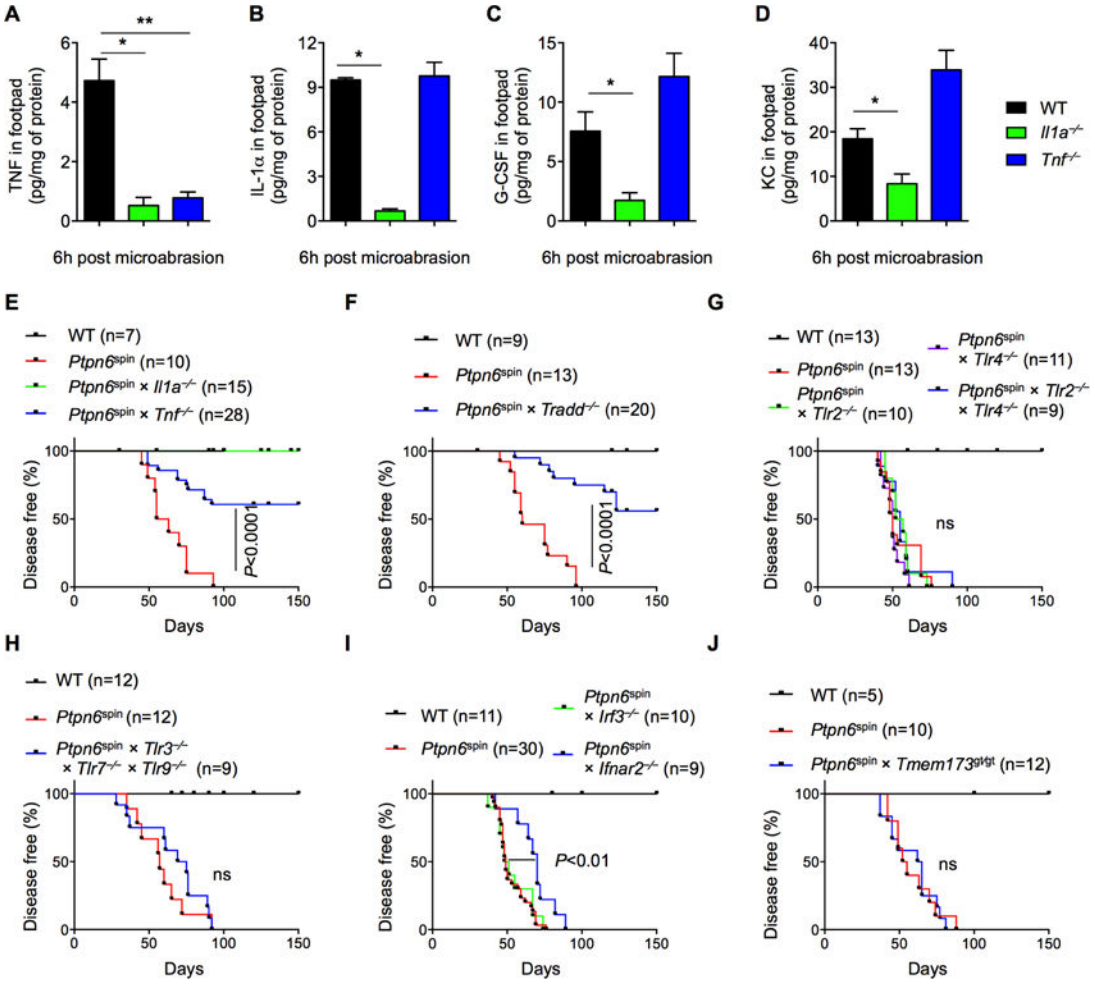

Figure 3. TNF and TRADD promote autoinflammatory disease in *Ptpn6*^{spin} mice. Please see also Figure S3

(A–D) Footpads of WT (n=5), *Il1a*$^{-/-}$ (n=4), and *Tnf*$^{-/-}$ (n=6) mice were microabrated, and the concentrations of TNF **(A)**, IL-1α **(B)**, G-CSF **(C)**, and KC **(D)** were measured in the footpads 6 hours post microabrasion.

(E–F) Disease curves of WT, *Ptpn6*^{spin}, *Ptpn6*^{spin} × *Il1a*$^{-/-}$, *Ptpn6*^{spin} × *Tnf*$^{-/-}$ **(E)**, *and Ptpn6*^{spin} × *Tradd*$^{-/-}$ **(F)** mice.

(G) Disease progression in *Ptpn6*^{spin}, *Ptpn6*^{spin} × *Tlr2*$^{-/-}$, *Ptpn6*^{spin} × *Tlr4*$^{-/-}$ and *Ptpn6*^{spin} × *Tlr2*$^{-/-}$ × *Tlr4*$^{-/-}$ mice.

(H) Disease progression in *Ptpn6*^{spin} and *Ptpn6*^{spin} × *Tlr3*$^{-/-}$ × *Tlr7*$^{-/-}$ × *Tlr9*$^{-/-}$ mice.

(I) *Ptpn6*^{spin}, *Ptpn6*^{spin} × *Irf3*$^{-/-}$ and *Ptpn6*^{spin} × *Ifnar2*$^{-/-}$ mice were observed for disease progression.

(J) *Ptpn6*^{spin} and *Ptpn6*^{spin} × *Tmem173*$^{gt/gt}$ mice were observed for disease progression.

Disease curves of *Ptpn6*^{spin} mice and the experimental *Ptpn6*^{spin} crosses were analyzed by Log-rank (Mantel-Cox) test. Mann-Whitney testing was used to determine the significance between the two groups analyzed **(A–D).** **P*<0.05, ***P*<0.01, ns=not significant.

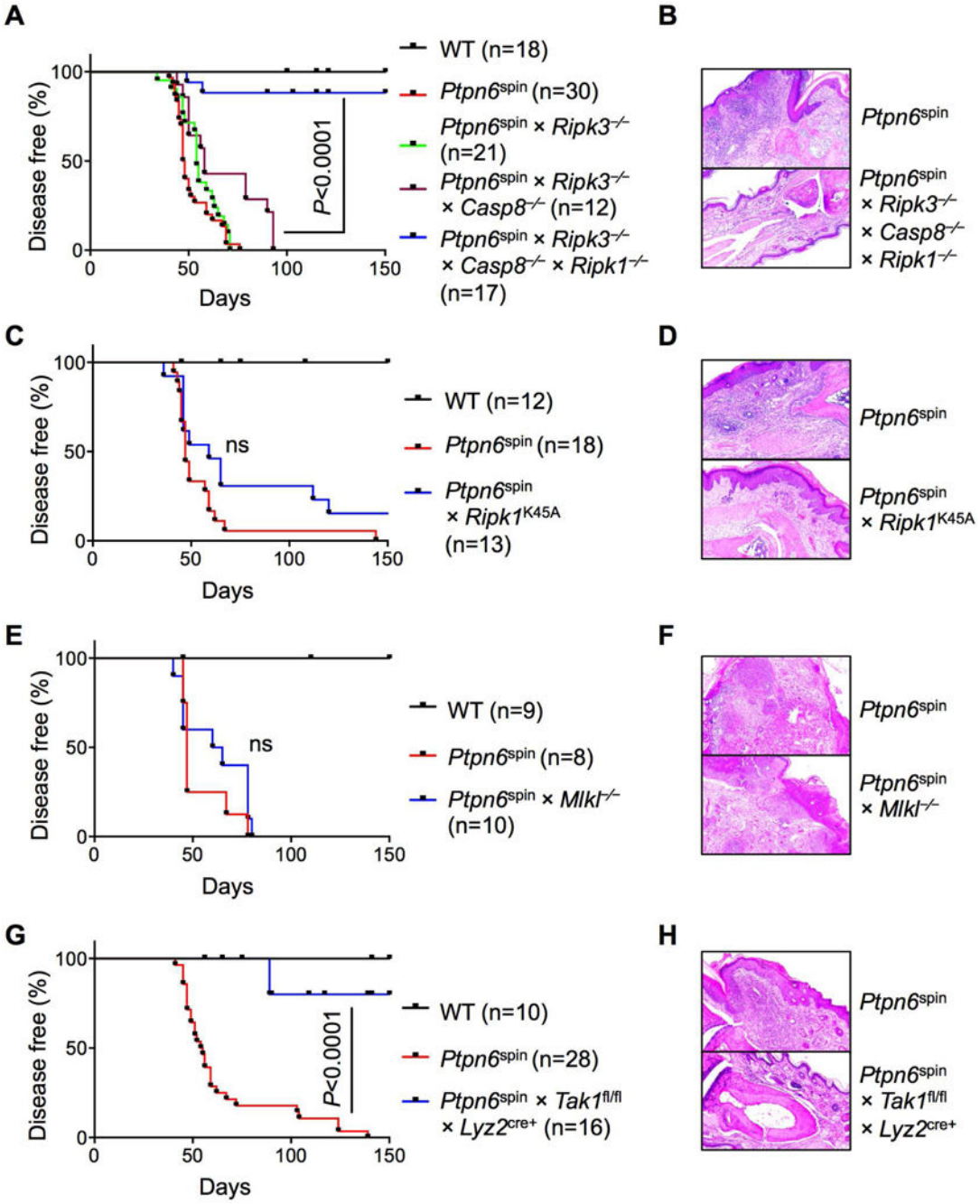

Figure 4. RIPK1 scaffolding function and TAK1 drive disease in *Ptpn6*^{spin} mice. Please see also Figure S3

WT, *Ptpn6*^{spin}, and *Ptpn6*^{spin} crosses were observed for disease progression.

(A–B) Disease curves **(A)** and H&E stain **(B)** of WT, *Ptpn6*^{spin}, and *Ptpn6*^{spin} × *Ripk3*$^{-/-}$ × *Casp8*$^{-/-}$ × *Ripk1*$^{-/-}$ mice.

(C–D) WT, *Ptpn6*^{spin}, and *Ptpn6*^{spin} ×*Ripk1*^{K45A} mice were observed for disease progression, **(C)** and H&E stain **(D)** of the footpads.

(E–F) Disease curves **(E)** and H&E stain **(F)** from WT, *Ptpn6*^{spin}, and *Ptpn6*^{spin} × *Mlkl*$^{-/-}$ mice.

(G–H) Disease curves **(G)** and footpad H&E stain **(H)** from *Ptpn6*^{spin} and *Ptpn6*^{spin} × *Tak1*$^{fl/fl}$ × *Lyz2*$^{cre+}$ mice.

The disease curves for *Ptpn6*^{spin} mice and the experimental group were analyzed by Log-rank (Mantel-Cox) testing. ns=not significant.

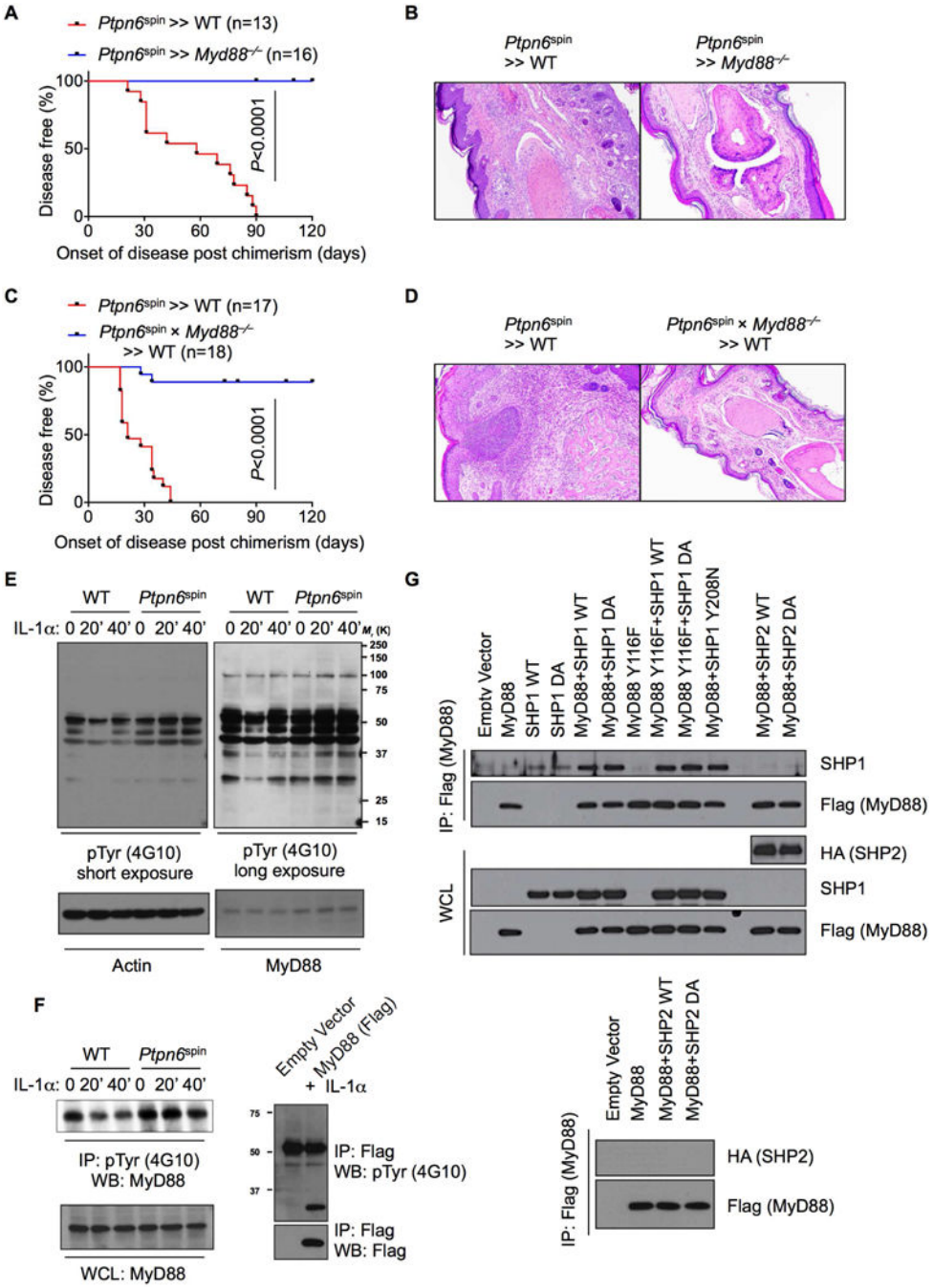

Figure 5. SHP1 regulates tyrosine phosphorylation of MyD88 to regulate skin disease

Disease progression and footpad inflammation in *Ptpn6*^{spin} chimera mice lacking MyD88 in either the hematopoietic or radioresistant compartment.

(A–B) Disease curves **(A)** and H&E staining of footpads **(B)** from *Ptpn6*^{spin} ≫ WT *and* *Ptpn6*^{spin} ≫ *Myd88*$^{-/-}$ chimeras.

(C–D) Disease curved **(C)** and H&E staining of footpads **(D)** from *Ptpn6*^{spin} ≫ WT *and* *Ptpn6*^{spin} × *Myd88*$^{-/-}$ ≫ WT chimeras.

(E) Myeloid cells from WT and *Ptpn6*^{spin} mice were stimulated with 20 ng/ml IL-1α for 20 or 40 minutes. Cell lysates were collected at the end of the experiment and probed with pan-phosphotyrosine (pTyr) antibody (Clone 4G10). Two different exposures (short and long) of the tyrosine phosphorylation blots are shown. Actin and MyD88 are used as protein loading controls.

(F) Cell lysates prepared as in **"E"** were immunoprecipitated by using pTyr antibody and probed for MyD88 to show tyrosine phosphorylation of MyD88 **(left panel).** Flag-tagged MyD88 was transfected in HEK 293 C6 cells and probed for tyrosine phosphorylation by using pTyr antibody after MyD88 immunoprecipitation **(right panel).**

(G) HEK293 C6 cells were co-transfected with indicated MyD88 and SHP1 constructs containing indicated proteins and the interaction of SHP1 and MyD88 were determined following MyD88 pull-down by Western blot **(upper panel).** HEK293 C6 cells were co-transfected with MyD88 and SHP2 and interaction of MyD88 and SHP2 were determined by Western blot **(lower panel).**

Disease curves in **(A)** and **(C)** were analyzed by Log-rank (Mantel-Cox) testing. All western blot data in **(E–G)** are representative of at least three independent experiments. $P<0.05$ is considered statistically significant.

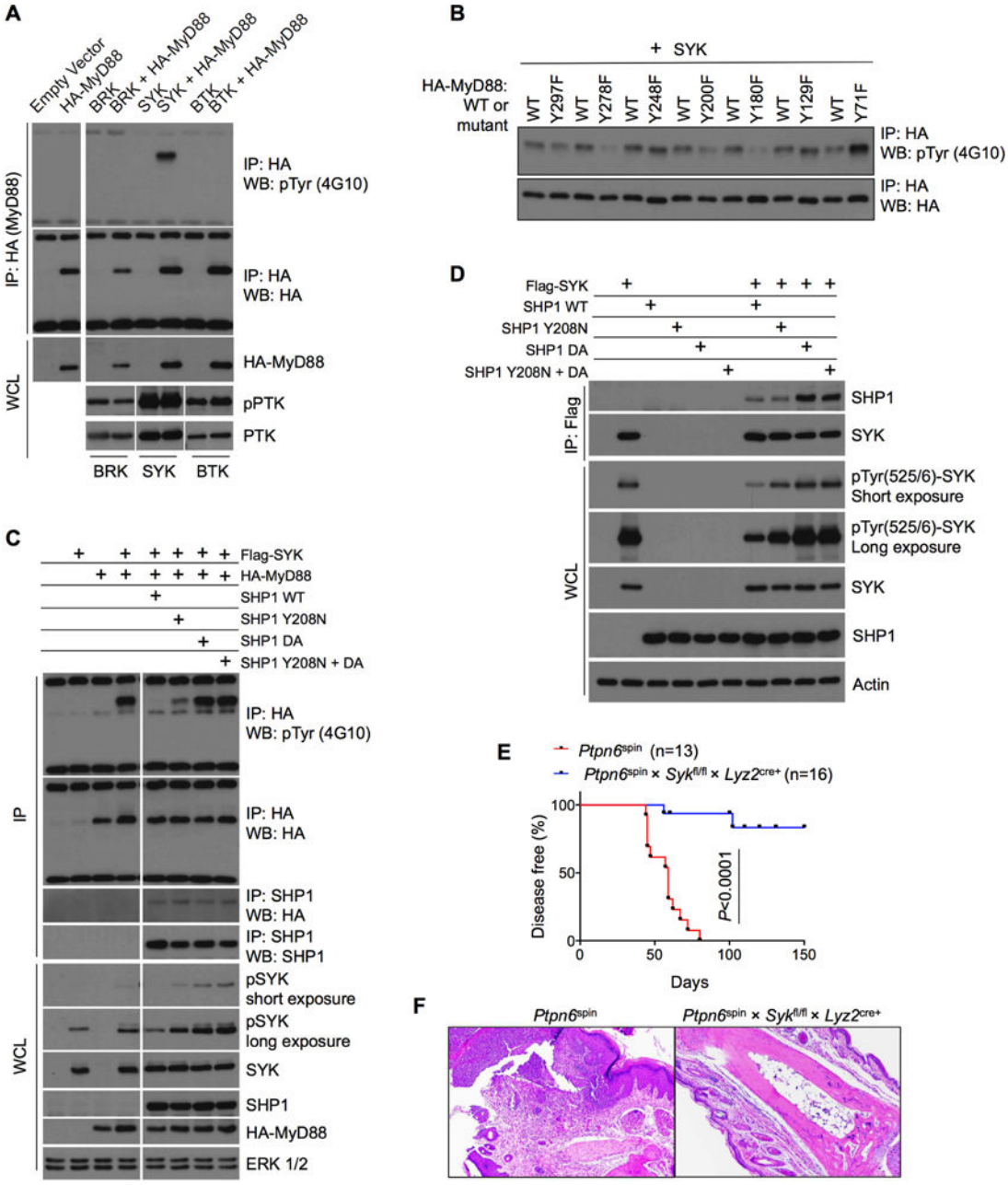

Figure 6. SYK promotes MyD88 phosphorylation to provoke inflammatory disease in *Ptpn6*^{spin} mice. Please see also Figure S4 and S5

(**A**) HA-tagged MyD88 was transfected, alone or together with PTKs (BRK, SYK or BTK) in 293T cells. Cell lysates were immunoprecipitated with anti-HA resin, and probed for tyrosine phosphorylation with 4G10. The expression of HA-MyD88 and PTKs were also probed, respectively, in whole cell lysates.

(**B**) WT and 7 YF mutants of HA-tagged MyD88 were co-transfected with SYK in 293T cells. Cell lysates were immunoprecipitated with anti-HA resin, and probed for tyrosine phosphorylation (4G10) and total HA-MyD88 pull-down.

(**C**) Indicated constructs were transfected in 293 C6 cell. Before harvest, cells were stimulated with IL-1α (20ngml) for 20 min. Cell lysates were immunoprecipitated with anti-HA resin, and probed for tyrosine phosphorylation (4G10) and total HA-MyD88 pull-down. Same lysates were also immunoprecipitated with anti-SHP1 antibody and probed for HA to assess the interaction between SHP1 (WT or mutants) and HA-MyD88. The expression of HA-MyD88, SYK and SHP1, as well as pSYK (pY525/6) was probed, respectively, in whole cell lysate extracts.

(**D**) FLAG-tagged SYK and SHP1 (WT or mutants) were transfected alone or together, as indicated, in 293 C6 cell. Before harvest, cells were stimulated with IL-1α (20ng/ml) for 20 min. Cell lysates were immunoprecipitated with anti-FLAG resin, and probed for SHP1 antibody to assess the interaction between FLAG-SYK and SHP1 (WT or mutants). The expression of SYK and SHP1, as well as pSYK (pY525/6) was probed, respectively, in whole cell lysates.

(**E–F**) Disease curves (**E**) and footpad H&E section (**F**) from $Ptpn6^{spin}$ and $Ptpn6^{spin} \times Syk^{fl/fl} \times Lyz2^{cre+}$ mice.

The disease curves for $Ptpn6^{spin}$ mice and the experimental group were analyzed by Log-rank (Mantel-Cox) testing.